On a minimizing movement for diffusion-generated interfacial motions

Elliott Ginder*

Graduate School of Natural Science and Technology
Kanazawa University, Japan

Seiro Omata
Kanazawa University, Japan

Karel Svadlenka
Kanazawa University, Japan

1   Introduction

A diffusion-based procedure for approximating interfacial motion by mean curvature was proposed by Bence, Merriman, and Osher in [6]. This algorithm, known as BMO, enjoys the ability to automatically treat topological changes of the phases, and is also very simple to implement.

We use the idea of the BMO to develop a method for volume-preserving multiphase motion by mean curvature. Our method inherits the nice features of the BMO, allows one to include arbitrary transport terms, and is also able to circumvent the well-known restrictions on the time and grid spacing used in its implementation. As volume-preserving motions tend to be slower than those of the non-constrained case, these restrictions pose an immediate issue to the development of such an algorithm. Until now, the volume-preserving BMO has been limited to the scheme introduced in [9]. Here, although careful choice of the initial conditions enables their method to capture the evolution of symmetric standard double bubbles, the number of phases is essentially limited to two.

We first reformulate the BMO process in terms of a single vector-valued heat equation. A minimizing movement, which is a vector-type *discrete Morse flow* [4], is then used to treat this problem. This method discretizes time and introduces a functional at each time step. The minimizers of these functionals are time-local approximations to the target problem and the variational nature of this approach then allows one to prescribe, via penalization, the volume of each phase. This aspect of our approach also benefits its computational implementation by its ability to automatically determine the configuration of the free boundaries (interfaces), while satisfying the prescribed volumes.

Section 2 recalls the original multiphase BMO algorithm and section 3 explains our reformulation. The possibility of additional transport terms and other constrained motions are touched upon in section 4, and the minimizing movement for our problem is given in section 5. The computational implementation of our method is explained in section 6 and section 7 shows the computational behavior our method for a six phase flow in the two dimensional setting. These motions can be thought of as describing the slow motion of bubbles (see Figure 4).

2   The original multiphase BMO

Given a collection of sets $E_i \subset \mathbf{R}^d$, $i = 1, ..., N$, where N denotes the number of phases, the BMO evolves the boundary of each set with velocities given by the mean curvature. A small time step Δt is decided, and the BMO convolutes a characteristic function of each set with the d-dimensional Gaussian kernel:

$$u^i(\Delta t, x) = (G_{\Delta t} * \chi_{E_i})(x) \tag{1}$$

where

$$G_s(x) = \frac{1}{(4\pi s)^{d/2}} e^{-\frac{|x|^2}{4s}}$$

and

$$\chi_{E_i} = \begin{cases} 1 & \text{if } x \in E_i, \\ 0 & \text{otherwise.} \end{cases}$$

The evolved interfaces are then obtained from the diffused characteristic functions in a step called *thresholding*:

$$E_i(\Delta t, x) = \{x : u^i(\Delta t, x) = \max_{j \neq i} u^j(\Delta t, x)\}. \tag{2}$$

Repeating the convolution and tresholding steps generates the sequence of time discrete approximations to the motion.

3   Reformulation of the BMO

We now introduce a reformulation of this algorithm in terms of a single vector-valued heat equation, which we consider in a bounded domain. As we will find, the variational aspect of our reformulation will permit us to consider an additional volume constraint on each phase.

Choosing a small time step Δt, we reformulate the BMO algorithm as finding a function $\mathbf{u} : \Omega \to \mathbf{R}^{N-1}$ solving a single vector-valued heat equation:

$$\begin{cases} \mathbf{u}_t = \Delta \mathbf{u} & \text{in } (0, \Delta t) \times \Omega \\ \frac{\partial \mathbf{u}}{\partial \nu} = 0 & \text{on } (0, \Delta t) \times \partial\Omega \\ \mathbf{u}(t = 0, x) = \mathbf{E}_0 & \text{in } \Omega, \end{cases} \tag{3}$$

where N denotes the number of phases, Ω is a bounded domain in $\mathbf{R}^d$, and the initial condition is defined by

$$\mathbf{E}_0(x) = \mathbf{p}_i \qquad \text{if } x \in E_i. \tag{4}$$

Here, $E_i \subset \Omega$ denotes the set corresponding to the ith phase, and $\mathbf{p}_i$ is the ith coordinate vector of a *regular simplex* in $\mathbf{R}^{N-1}$ (see Figure 2), $i = 1, ..., N$. We remark that, when $N = 2$, the vector-valued heat equation is scalar and agrees with the original BMO.

At time Δt, in a process called *thresholding*, each region E_i is evolved:

$$E_i(\Delta t) = \{x \in \Omega : \mathbf{u}(\Delta t, x) \cdot \mathbf{p}_i \geq \mathbf{u}(\Delta t, x) \cdot \mathbf{p}_k, \forall k \neq i\}. \tag{5}$$

The initial condition $\mathbf{E}_0$ is then updated by (4) and the procedure is repeated.

Moreover, it can be shown that the above process is equivalent to the original BMO algorithm for multiphase motion by mean curvature. One need only consider the scalar valued function

$$w^j(t, x) = \frac{N-1}{N} \left(\mathbf{u} \cdot \mathbf{p}^j + \frac{1}{N-1} \right). \tag{6}$$

Using the fact that $\mathbf{u}$ solves (3), together with the properties of the vectors from the regular simplex:

$$\mathbf{p}^i \cdot \mathbf{p}^j = \begin{cases} 1 & \text{if } i = j, \\ \frac{-1}{N-1} & \text{otherwise,} \end{cases}$$

it is readily seen that the initial conditions and the PDE governing the evolution of w^j, as well as the thresholding (5) are consistent with those of the original BMO.
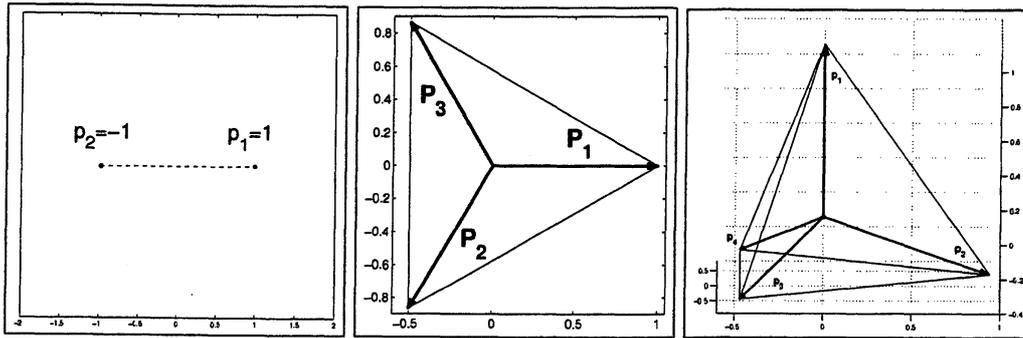
Figure 1: (Left) The 2-phase regular simplex. (Center) The 3-phase regular simplex. (Right) The 4-phase regular simplex.

4 Transport and volume preservation

Convolution with the Gaussian kernel in the two-phase case has been shown to yield interfacial motions with velocity given by mean curvature [1, 3]. In the same way, one can formally show that threshold dynamics governed by

$$u_t = \Delta u + \frac{f(x)}{\sqrt{4\pi t}} + \lambda \mathcal{H}^{d-1} \lfloor_{\partial\{u>0\}}, \tag{7}$$

where $\lambda(t)$ is a function of time and $\mathcal{H}^d$ denotes the d-dimensional Hausdorff measure, yields interfacial motions of characteristic functions with velocity:

$$v = -\kappa + f + k.$$

Here κ denotes the mean curvature, f is a given transport term, and k is a function of time only. For more on the constrained two-phase problem with transport, see [5].

Thus volume-preserving motions under transport are reduced to finding a Lagrange multiplier λ, as well as the location of the free boundary, so that the constraint is achieved. In the case $f = 0$, we remark that λ should be found so that k becomes the average mean curvature of the interface. Nevertheless, we will see that the variational nature of our algorithm is able to evade the need to specifically determine such multipliers and automatically determines the position of each interface.

5 The minimizing movement

In treating the volume constrained motions, the reformulated BMO process (stated in terms of a vector-valued heat equation) is approximated by use of a minimizing movement. A discretization in time is used to build approximate solutions by successively minimizing time-dependent functionals; hence this setting conveniently allows one to include constraints via penalization. Each minimizer then corresponds to the solution of an vector-valued elliptic problem with Lagrange multipliers appearing on the free boundaries.

Namely, we use a vector-type *discrete Morse flow* to treat our problem. We choose a large positive integer K which determines the time step of the flow, $h = \Delta t/K$. Using (4), we set an initial function $\mathbf{w}_0 = \mathbf{E}_0$. Then for each $n = 1, ..., K$ we minimize the following functional over $H^1(\Omega; \mathbf{R}^N)$:

$$\mathcal{J}_n(\mathbf{w}) = \int_\Omega \left(\frac{|\mathbf{w} - \mathbf{w}_{n-1}|^2}{2h} + \frac{|\nabla \mathbf{w}|^2}{2} - \frac{\mathbf{w} \cdot \mathbf{f}}{\sqrt{4\pi nh}} \right) dx, \tag{8}$$

where **f** denotes a vector in $\mathbf{R}^{N-1}$ of source terms.

To evolve the interface for a time T, our method takes $M = T/\Delta t$ and, beginning with the initial condition $\mathbf{u}_0 = \mathbf{w}_0$, repeats the following for $m = 1, ..., M$:

1. Set $\mathbf{w}_0 = \mathbf{u}_{m-1}$.

2. For $n = 1, ..., K$, compute $\mathbf{w}_n$ to be the minimizer of $\mathcal{J}_n(\mathbf{w})$ over $H^1(\Omega; \mathbf{R}^N)$.

3. Update each region E_i using (5), $i = 1, ..., N$.

4. Set $\mathbf{u}_m = \mathbf{E}_0$, given by (4).

The sequence of functions $\{\mathbf{u}_m\}_{m=0}^M$ then gives an approximation to the (unconstrained) multi-phase motion. Figure 2 shows the basic characteristics of the method for a four-phase problem, but see section 7 for a clarification of the initial condition.

In treating volume-constrained motions, one can now see that the minimization aspect of our reformulated algorithm should allow the inclusion of volume constraints via penalization. For example, denoting the prescribed volume of region E_k by V_k, the energy functional can be modified:

$$\mathcal{F}_n(\mathbf{w}) = \mathcal{J}_n(\mathbf{w}) + \frac{1}{\epsilon} \sum_{k=1}^N |V_k - meas(E_k^{\mathbf{w}})|^2. \tag{9}$$

Here $\epsilon > 0$ is a small penalty parameter and the areas corresponding to **w** are obtained from the sets

$$E_k^{\mathbf{w}} = \{x \in \Omega : \mathbf{w} \cdot \mathbf{p}_k \geq \mathbf{w} \cdot \mathbf{p}_i, \forall i \neq k\}.$$

See section 7 for an illustration of our method applied to the case of volume-constrained motions for a six-phase problem.
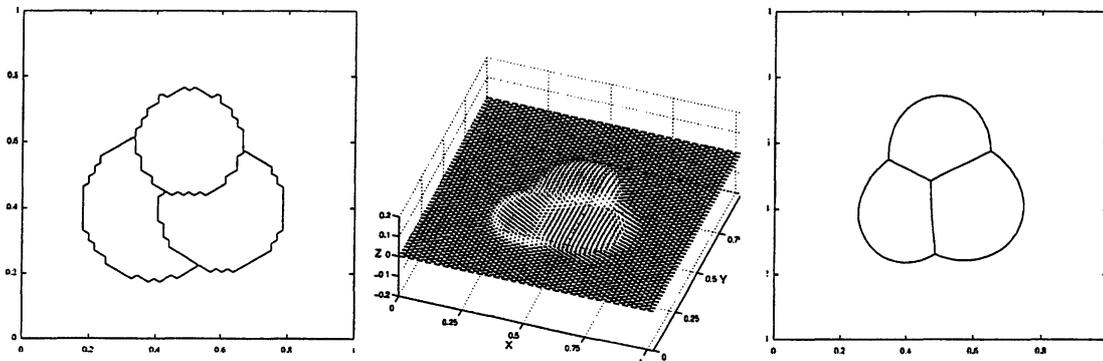
Figure 2: (Left) The initial condition. (Center) An instant in time of the vector-valued heat equation. (Right) The corresponding interfaces.

6   Implementation of the method

The numerical implementation of our method uses the finite element method to approximate the functional values (9), and minimizers are found by gradient descent. The domain is triangulated into a finite number of elements, over which we assume that the function is continuous and a

linear interpolation between node vectors, and the approximate value of the functional (9) is then given by the sum of the integrals over each element. The solution to vector-type equation of (7) is thus approximated by successive minimizations of (9) until arriving at the thresholding step. As noted in the introduction, simple thresholding by (2) is known to inhibit the motions obtained by computing with the BMO algorithm (see also, [2]). We now explain our approach to alleviating these troubles.

Before thresholding, the interface is piecewise linear and continuous, and, in the volume-preserving case, approximately satisfies the prescribed area constraint. However, applying the original formulation of the thresholding (2) at each node location would then reduce the smoothness of the interface, as well as alter the enclosed area. This causes two difficulties, the most significant being that, upon proceeding to the next minimizer, the interface may fail to move (thus becoming stationary). That is, since each evolution is obtained via the heat equation, the diffusion process must proceed long enough so that the grid resolution resolves the movement of each interface across the elements. Additionally, due to the constraints on the area of each phase, the normal velocity of the interfaces tends to be much slower than motion by uncon-strained mean curvature, especially near the stable state. Therefore this issue is particularly relevant to our current problem. The second issue is that the enclosed areas cannot be preserved with sufficient precision after this thresholding.

We are able to overcome these issues by use of the following. Just prior to the threshold step (i.e., $Kh = \Delta t$), we indicate the elements that span interfaces by e_j^*, record the interfacial geometry, and then threshold. Upon the next minimization, whenever we come to an indicated element, we recall the geometry of the interfaces and compute the value by means of a trian-gulation of the element. In particular, the value over an indicated element is obtained by the values over a set of convex polygons, each denoted by R_i. These regions are determined by the element nodes and the intersection of the recorded interfaces with the element edges (see Figure 3):

$$R_i = \{x \in e_j^* : \mathbf{u}_K \cdot \mathbf{p}_i \geq \mathbf{u}_K \cdot \mathbf{p}_l, \forall l \neq i\}.$$

For a candidate minimizer $\mathbf{u}$, the value of the time term in the functional (8) is then computed:

$$\int_{e_j^*} \frac{|\mathbf{u} - \mathbf{u}_{n-1}|^2}{2h} dx = \sum_{k=1}^{N} \int_{R_k \cap e_j^*} \frac{|\mathbf{u} - \mathbf{p}_k|^2}{2h} dx, \tag{10}$$

and the contributed areas for the penalty terms are accumulated:

$$meas(e_j^* \cap E_k) = meas(R_k). \tag{11}$$

By such an approach, we are able to realize interfacial motions whose configuration and precision of enclosed area are not influenced by truncations.

7   Computation of a six phase flow

We show the result of our algorithm applied to a volume-constrained six-phase flow. The domain $\Omega = [0,1] \times [0,1]$ is triangulated into approximately 5500 elements, $f \equiv 0$, $h = 5 \times 10^{-5}$, and $K = 10$ ($\Delta t = 5 \times 10^{-4}$). The mesh is nearly uniform so that most elements have area approximately equal to 10^{-4}. A penalty of the form shown in (9) is added for each phase and its parameter is $\epsilon = 10^{-6}$.

Six phases are positioned throughout the domain. Since we use $\mathbb{P}_1$ Lagrange finite elements, after assigning one of the six vectors $\mathbf{p}_i \in \mathbf{R}^5$ (see Figure 1) to the proper node location and
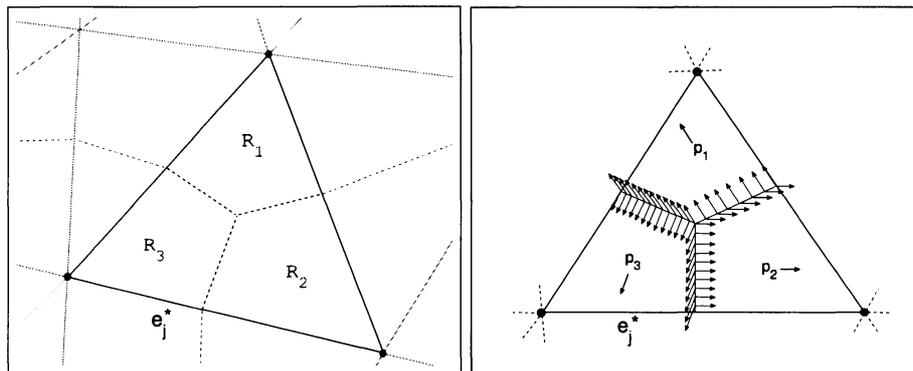
Figure 3: (Left) Three regions inside an indicated element. (Right) Vectors inside the element after thresholding.

detecting the interface, we have the initial location of the interface as shown in Figure 4. We remark that, although the initial interface appears jagged, the geometry is exact under or assumptions on the data. Moreover, this does not present an issue to any of the computations.

The physical interpretation is as follows. We configure five bubbles into the shape shown in Figure 4 and then let them evolve (the sixth phase is represented by their surrounding region). The bubbles quickly smooth themselves and finally come to a rest in their stable configuration. By examining the data, we note that the so-called symmetric Herring conditions (junctions meeting at 120°) appear to be satisfied at junctions during the evolution.

We again mention that the process described in (10) is essential in computing these motions. Indeed, as the volume-preserving interfacial velocities tends to be slower than motion by mean curvature flow, the well-known time and grid spacing restrictions of the BMO become particularly relevant. Nevertheless, our method of recalling the interfacial geometry after thresholding allows us to avoid such complications, and can also be used for the non-constrained BMO with the same result. That is, one can choose the parameters so that the original BMO becomes stationary, but for which ours does not. Moreover, numerical tests suggest that our approach does not alter the characteristics of the target motion.
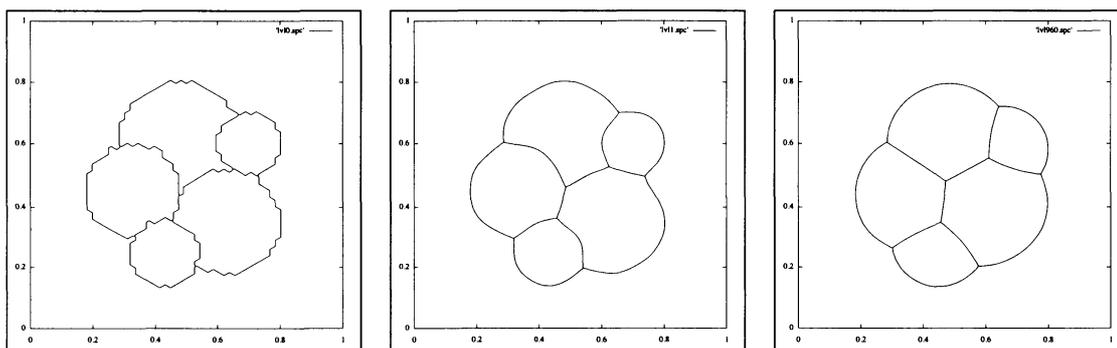
Figure 4: The initial condition, evolution after Δt, and the stable configuration.

8 Conclusion

The BMO algorithm was reformulated in terms of a vector-type discrete Morse flow and we investigated its computational properties. It was found that the variational nature of this ap-

proach allows one to consider constraints via additional penalty terms. The energy functionals were thus modified to include penalties, from which a multiphase volume-preserving problem was investigated numerically.

By detecting the precise locations of the interfaces (under the finite element assumptions) we are able to compute the area of each phase at a high precision and thus impose the volume constraints. This geometric information is then used to partition the elements that straddle the interfaces and for searching for the minimizer of the functional after thresholding. This approach was found to alleviate the BMO's standard restrictions on the spatial and time-step resolutions, for both the constrained and non-constrained problems.

In closing, we remark that it would be interesting to investigate our algorithm in relation to the recent threshold dynamics utilizing signed distances functions [2], and to consider its position in applications.

References

[1] Barles G., Georgelin C., "A simple proof of convergence of an approximation scheme for computing motions by mean curvature" *SIAM Journal of Numerical Analysis*, 32 (2) (1995), pp. 484-500.

[2] Esedoglu S., Ruuth S., Tsai R., "Diffusion Generated Motion using Signed Distance Functions" *J. Comp. Phys.*, 229 (4) (2010), pp. 1017-1042.

[3] Evans L. C., "Convergence of an algorithm for mean curvature motion" *Indiana University Mathematics Journal*, 42 (1993), pp. 533-557.

[4] Ginder E., "Construction of solutions to heat-type problems with time-dependent volume constraints" *Advances in Mathematical Sciences and Applications*, 20 No. 2 (2010), pp. 467-482.

[5] Ginder E., Omata S., Svadlenka K., "A variational method for diffusion-generated area-preserving interface motion" *Theoretical Applied Mechanics Japan*, 60 (2011), pp. 267-272.

[6] Merriman B., Bence J. K., Osher S. J., "Motion of Multiple Junctions: A Level Set Approach" *J. Comp. Phys.*, 112 (1994), pp. 334-363.

[7] Osher S., Sethian J. A., "Fronts propagating with curvature-dependent speed: Algorithms based on Hamilton-Jacobi formulations" *J. Comp. Phys.*, 79 (1988), pp. 12-49.

[8] Ruuth S. J., "Efficient Algorithms for Diffusion-Generated Motion by Mean Curvature" *J. Comp. Phys.*, 144 (1998) pp. 603-625.

[9] Ruuth S. J., Wetton B. T. R., "A Simple Scheme for Volume-Preserving Motion by Mean Curvature" *J. Sci. Comp.*, 19 (2003), pp. 373-384.